Exciton-polariton propagation in AlGaN/GaN quantum-well waveguides probed by time-resolved photoluminescence

T. N. Oder, J. Li, J. Y. Lin, and H. X. Jiang[a)]
Department of Physics, Kansas State University, Manhattan, KS 66506-2601

ABSTRACT

The propagation properties of light in AlGaN/GaN multiple-quantum-well (MQW) waveguides have been studied by time-resolved photoluminescence (PL) spectroscopy. The waveguides were patterned with fixed width of 0.5 μm but orientations varying from -30° to 60° relative to the a-axis of GaN by electron-beam lithography and inductively-coupled plasma (ICP) dry etching. The peak position and line-width of the emission peak were found to vary systematically with orientations of the waveguides and followed the six-fold symmetry of the wurtzite structure. This is explained in terms of anisotropy of the exciton/carrier diffusion coefficient along the different crystal orientations of the semiconductor materials. We also observed a remarkable decrease in the PL intensity as well as increase in time delay of the temporal response as the location of the laser excitation spot on the waveguide is varied. These observations can be understood in terms of exciton-polariton propagation in the waveguides. The speed of generated polaritons with energy corresponding to the well transitions in the waveguides was determined from the time delay of the temporal response to be approximately $(1.26 \pm 0.16) \times 10^7$ m/sec. The optical loss in the waveguides was determined to be about 5 - 8 cm^{-1} for different excitation intensities. The implications of these results to waveguiding in optical devices based on the III-nitride semiconductors are discussed.

Keywords: AlGaN/GaN quantum wells, waveguides, submicron, time-resolved PL, exciton-polariton

1. INTRODUCTION

The group III-nitride semiconductors consisting of AlN, GaN, InN and their alloys have been intensively studied as they are very promising materials for many optoelectronic device applications such as blue-green and UV light emitting diodes (LEDs), laser diodes (LDs), UV solar blind detectors, and high-temperature/high-power electronic devices [1]. However, not so many studies have been done on submicron structures in the III-nitrides due to the difficulties involved in fabrication and characterization. When structural dimensions are reduced to submicron sizes, significant changes in properties such as carrier and photon dynamics of the semiconductor structures will result. There is therefore a great need to study low-dimensional optical and electronic systems such as waveguide structures especially in the III-nitride semiconductors in order to elucidate the basic physics governing the optical properties in submicron size structures. These may open doors for new applications as well as contribute to the improvement of the design of existing devices where such structures are used. There is also interest in investigating the potential of the III-nitrides for waveguide materials.

Our group has previously fabricated structures of a few μm in dimension using photolithography [2–6]. It is difficult to achieve structures of dimensions less than 1 μm in the III-nitride materials using standard photolithography. Also, because the III-nitrides are hard materials, the usual method to achieve pattern-transfer is by high-density plasma etching. Here, we summarize the results from the fabrication and optical study of submicron waveguide patterns based on AlGaN/GaN multiple quantum wells (MQW). Our results reveal that the peak position and line-width of the emission peak vary systematically with the waveguide orientations. We explain these observations in terms of anisotropy of carrier or exciton diffusion coefficient in a quasi one-dimensional (1D) structure. In addition, we observed a systematic decrease of the emission intensity as the location of the incident laser spot is moved further away from one end of the waveguide. We determined the optical loss in the waveguides to be 5 - 8 cm^{-1} for different excitation intensities. From the temporal response, we have determined the propagation speed of light in the waveguide, with energy corresponding to the well transitions in the MQW, to be $(1.26 \pm 0.16) \times 10^7$ m/sec. No results for light propagation in waveguides based on these materials have previously been obtained to our knowledge. These results are explained in terms of the propagation properties of exciton-polaritons in the waveguides.

Ultrafast Phenomena in Semiconductors VI, Kong-Thon F. Tsen, Jin-Joo Song, Hongxing Jiang, Editors, Proceedings of SPIE Vol. 4643 (2002) © 2002 SPIE · 0277-786X/02/$15.00

Downloaded From: http://proceedings.spiedigitallibrary.org/ on 05/01/2014 Terms of Use: http://spiedl.org/terms

2. EXPERIMENT

The AlGaN/GaN MQWs were grown by metalorganic chemical vapor deposition (MOCVD). The metalorganic sources used were trimethylgallium (TMG) and trimethylaluminum (TMAl). Ammonia gas was used as the nitrogen precursor. A 300 Å low temperature GaN buffer layer was first deposited on the sapphire substrate, followed by deposition of 1.0 μm GaN layer. Thirty periods of $Al_{0.2}Ga_{0.8}N$ /GaN were then grown between a pair of 200 Å thick $Al_{0.2}Ga_{0.8}N$ cladding layers. To provide lateral confinement, the waveguides were defined by electron-beam lithography technique. Following the standard de-grease clean, 2 drops of negative resist (PN-114, a novalak-based polymer from Clariant Corporation) were spun at 8,000 rpm for 30 seconds to yield an estimated resist thickness of about 1.2 μm. A pre-exposure oven bake was carried out at 120 °C for 30 min. The electron-beam used during the pattern writing was accelerated at 35 kV with a probe-current of 5 pA and an area dose of 5 $\mu C/cm^2$ using the LEO 440 scanning electron microscopy system (SEM). A post-exposure hot-plate bake was carried out at 105 °C for 5 min followed by developing for 90 sec in dilute aqueous alkaline solution (AZ 400K). The defined patterns were transferred to the sample by inductively coupled plasma (ICP) etching. Dry etching was done at 300 watts for 1 min, which resulted to an etch-depth of about 0.75 μm. The resist used not only maintained submicron definition of patterns, but also held through the etching process. Arrays of waveguide patterns occupying 500 μm x 500 μm field with a center-to-center separation of 1 mm were defined. The width and length of each waveguide were fixed at 0.5 μm and 500 μm respectively, with a spacing of 15 μm from each other. The orientation of the waveguides in each array group was varied from -30° to 60° relative to the a-axis of GaN. For comparison purpose, a region of size 500 μm x 500 μm was defined and left unpatterned in the sample. Low temperature (10 K) photoluminescence (PL) spectra were measured using laser spectroscopy system with an average output power of about 20 mW, tunable photon energy up to 4.5 eV and a spectral resolution of about 0.2 meV. Details of the laser system are described elsewhere [7]. The sample was placed normal to the incident light and the emitted photons were collected from a direction parallel to the sample surface. The emitted photons were dispersed using a 1.3 m monochromator with a photomultiplier tube (PMT) detection system. For time-resolved measurements, a streak camera detection system with time resolution of 2 ps was used.

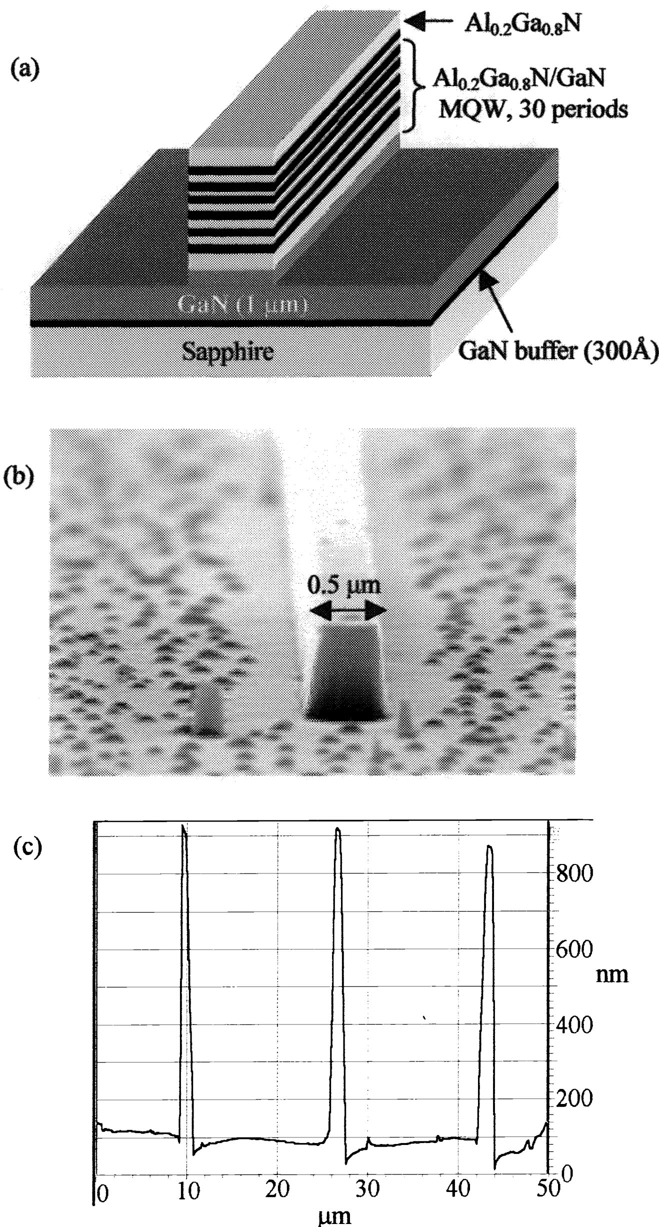

Fig. 1(a) Schematic diagram of the AlGaN/GaN MQW waveguide structure. (b) The scanning electron microscope (SEM) image and (c) a 2D line profile of the atomic force microscope (AFM) image of the waveguides.

3. RESULTS AND DISCUSSIONS

3.1 Orientation dependence

Fig. 1 (a) shows the schematic diagram of the waveguide while Fig. 1 (b) and (c) shows the scanning electron microscope (SEM) image and a 2D profile from the atomic force microscope (AFM) image of the waveguide, respectively. The width of the waveguides was about 0.5 μm as targeted and the etched surfaces of these structures were found to be quite smooth with excellent uniformity along the length of the waveguides.

Downloaded From: http://proceedings.spiedigitallibrary.org/ on 05/01/2014 Terms of Use: http://spiedl.org/terms

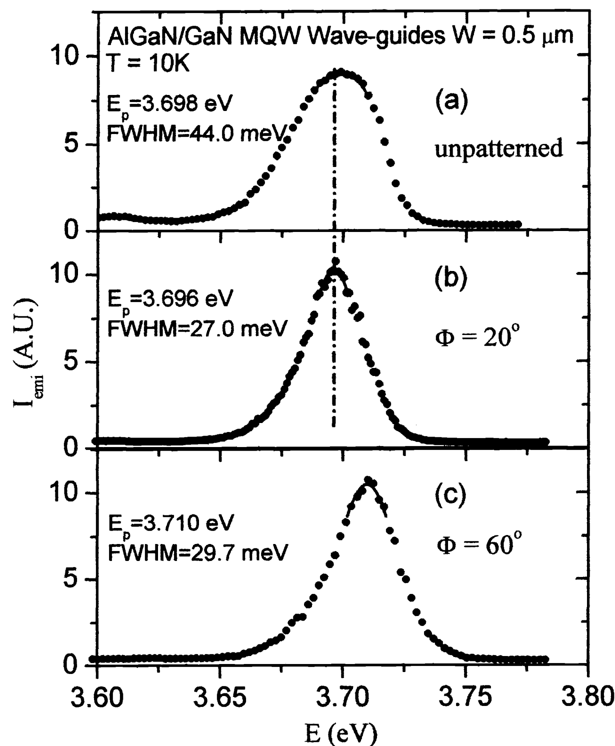

Fig. 2. Low temperature (10 K) cw PL spectra from AlGaN/GaN MQW waveguides of different line orientations. For clarity, we only show (a) the PL spectrum from an unpatterned portion of the sample and the PL spectra from waveguides oriented at (b) 20° and (c) 60°.

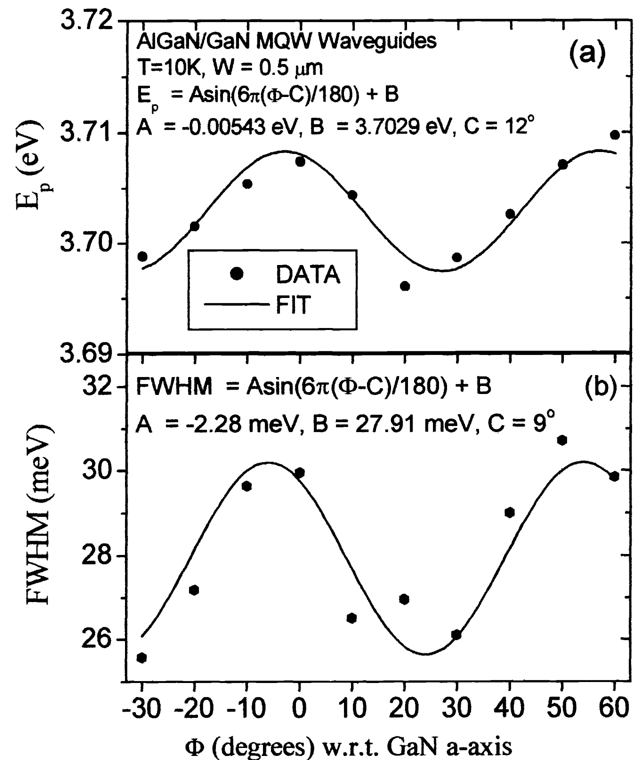

Fig. 3. Variation of (a) the spectral peak positions (E_p) and (b) full width at half maximum (FWHM) of the PL emission line at 10 K. The solid line is the sinusoidal fit of the data with 6-fold symmetry of hexagonal structure.

The resulting etch-depth of 0.75 μm ensured that the waveguides were etched through the AlGaN/GaN MQW and into the underlying GaN layer. For studies on the orientation dependence, the AlGaN/GaN MQW sample used had an AlGaN barrier width of 50 Å and a GaN well width of 12 Å. The sample was placed normal to the incident light focused to a spot size of about 15 μm at the middle of each array of waveguides and the emitted photons were collected from a direction parallel to the sample surface.

The PL spectra from the unpatterned portion of the sample and from two waveguides oriented at 20° and 60° are shown in Fig. 2 (a), (b) and (c) respectively. Only these three representative spectra are shown here for clarity. The emission peaks in these spectra are attributed to localized exciton recombination in the well regions of the waveguide structures. The line width of the spectrum from the unpatterned region is much broader than that of the spectrum from the waveguides. This difference will be explained later. The PL peak position, E_p, and full width at half maximum (FWHM) depend on the orientation, as can be seen in Fig. 2 (b) and (c). E_p and FWHM of the emission line versus the waveguide orientation (ϕ) relative to the a-axis of GaN are shown in Fig. 3 (a) and (b), respectively. As shown, there is a definite periodicity of 60° in E_p and FWHM, both varying sinusoidally as $A\sin[6\pi(\Phi-C)/180] + B$, where A, B and C are variables. E_p and FWHM are both maximum for orientations roughly parallel to 0° or 60° and both minimum for orientations roughly parallel to -30° or 30°. Between the two extremes, E_p changes by about 11 meV while FWHM changes by about 4.6 meV.

Kapolnek et al [8] investigated the orientation on the morphology and growth rates of lateral epitaxial overgrowth (LEO) of GaN. It was found that lines oriented parallel to 30° relative to the a-axis of GaN had low lateral to vertical growth rate and resulted to triangular wedge cross sections. Lines parallel to 0° or 60° however had high lateral to vertical growth rate ratios. Asai [9] also observed a very similar trend in the anisotropy of lateral growth in GaAs. These observations of the 60° periodicity as well as our results shown in Fig. 3 are expected from the hexagonal symmetry of the nitride materials.

The major cause of variation in E_p and FWHM in semiconductor MQW systems is localization effects caused by fluctuations in the well width and alloy composition [10,11]. In the AlGaN/GaN MQW that we have studied here, the well

Downloaded From: http://proceedings.spiedigitallibrary.org/ on 05/01/2014 Terms of Use: http://spiedl.org/terms

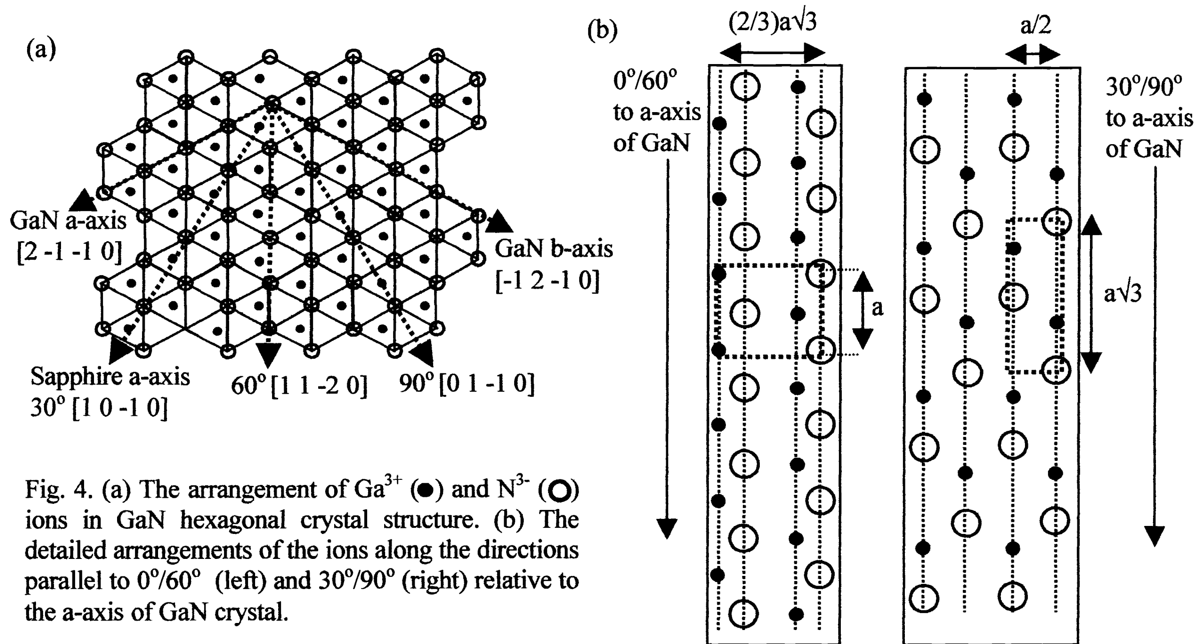

Fig. 4. (a) The arrangement of Ga^{3+} (●) and N^{3-} (O) ions in GaN hexagonal crystal structure. (b) The detailed arrangements of the ions along the directions parallel to 0°/60° (left) and 30°/90° (right) relative to the a-axis of GaN crystal.

region is a binary semiconductor (GaN) for which localization effects would be due only to well width fluctuations. However, we expect well width fluctuations to be the same for these waveguide structures irrespective of their orientations as their widths are equal. The diffusion process in the unpatterned region of the sample can be regarded as two-dimensional while that in each waveguide as quasi one-dimensional. An unpatterned region of the sample whose PL spectrum is shown in Fig. 2 (a) will have more low energy sites compared to the waveguide structures, since a much larger area is involved for the unpatterned region compared with the waveguides. From the PL spectra of another set of waveguides with different widths but fixed orientation, the spectral peak position E_p of the emission line was observed to shift towards lower energy as the waveguide width was increased (not shown). This behavior is consistent with our interpretation that more low energy sites are available in wider waveguides. The observed anisotropic optical properties with the 6-fold symmetry in the nitride quantum well plane can be understood by the anisotropic diffusion of photo-excited carriers and excitons for waveguides along different orientations. For fixed excitation laser intensity, due to the band filling effect, carrier or exciton density will be higher for the case of either lower diffusion coefficient or less potential fluctuation.

In Fig. 4 (a), we show the schematic arrangements of Ga^{3+} and N^{3-} ions in hexagonal GaN, described more fully by Kung at al [12]. The arrangements of the ions along the directions parallel to 0°/60° and -30°/30° are specifically shown in Fig. 4 (b). The a-axis of GaN is shifted 30° with respect to the a-axis of sapphire. Waveguides oriented along -30°/30° (where E_p and FWHM are minimum) and 0°/60° (where E_p and FWHM are maximum) have the following differences in crystal arrangements: Firstly, the number of ions per unit length in the -30°/30° line is greater than that along the 0°/60° line by a factor of 10:9. Secondly, the lateral termination of the waveguides for the -30°/30° line is composed of both Ga and N ions while that of the 0°/60° line is either Ga or N. Thirdly; the width covered by 4 columns of ions is larger in the -30°/30° direction than in the 0°/60° direction. These differences could be the source of the anisotropy of the exciton/carrier diffusion coefficient in the quasi-1D waveguide structures. At 0°/60° orientations, there is slow carrier or exciton diffusion leading to band-filling effect with the result that E_p and FWHM are both maximum. Faster carrier/exciton diffusion occurs along the -30°/30° resulting in E_p and FWHM both being minimum. The most intriguing result we obtained above is that there is a difference in optical property of submicron structures, shown by the periodic variation in the peak energy E_p and FWHM of the spectra from MQW waveguides at different crystalline orientations. This difference is more pronounced in smaller structures. The major implication of this result is that in photonic and electronic devices where structures of submicron sizes are involved, there will be differences in exciton or carrier dynamics. The differences arising from the choice of orientation will result in significant effects in the associated devices. Such devices include field effect transistors (FETs), optical waveguides, photodetectors and ridge-guide laser diodes. Therefore in the design of these devices, proper attention must be paid in the choice of the orientation of the associated submicron structures.

Downloaded From: http://proceedings.spiedigitallibrary.org/ on 05/01/2014 Terms of Use: http://spiedl.org/terms

3.2 Exciton-polariton propagation

For studies on exciton-polariton propagation, the incident laser beam was focused to a spot size of about 2 μm on a single waveguide using a UV transmitting objective lens of focal length 3 mm. The AlGaN/GaN MQW sample used had thirty periods of AlGaN barrier of width 50 Å and a GaN well of width 24 Å. The sample was placed normal to the incident light and the emitted photons were collected from a direction parallel to the sample surface, as schematically shown in Fig. 5. The distance d (μm), from the edge of the waveguide closest to the collecting slit of the monochromator, defines the position of the incident excitation laser spot focused on the waveguide. Fig. 6 shows the PL spectra collected under laser excitation at three different positions of a waveguide lined perpendicular to the collecting slit of the monochromator. The emission line at 3.484 eV is from the underlying GaN epilayer exposed after dry etching as shown schematically in Fig. 1 (a). The integrated intensity at this emission line is approximately the same for the different values of d. The emission line at 3.585 eV is attributed to the localized exciton recombination in the quantum well regions of the waveguide structures. This peak position is

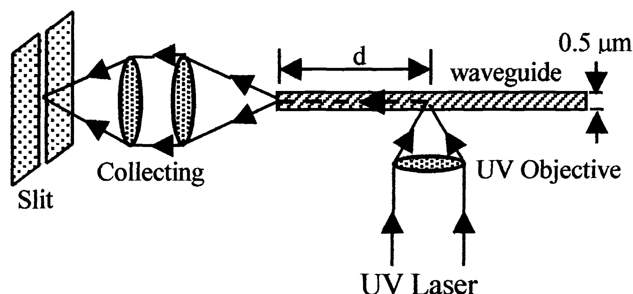

Fig. 5. Schematic diagram showing set-up of laser excitation for probing the propagation properties of exciton-polaritons in the AlGaN/GaN MQWs.

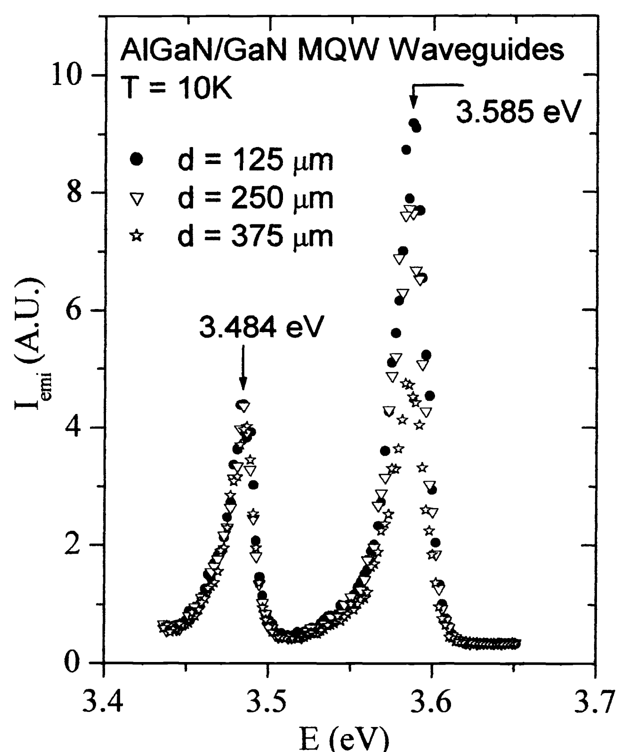

Fig. 6. Low temperature (10 K) cw PL spectra under laser excitation from three different positions, d on the AlGaN/GaN MQW waveguides lined perpendicular to the collecting slit of the monochromator. The peak at 3.484 eV is from the surrounding GaN exposed by etching and the peak at 3.585 eV is from the exciton recombination in the well regions of the waveguide structure.

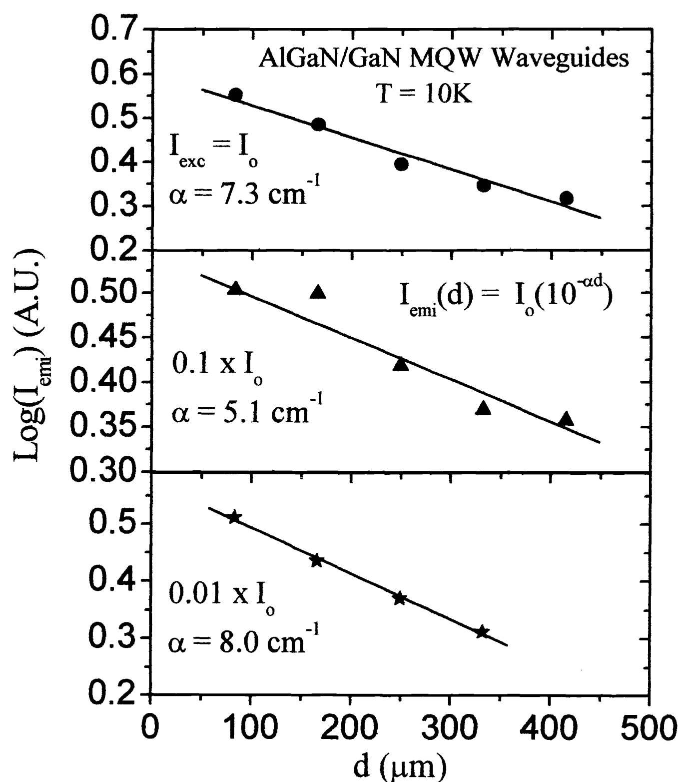

Fig. 7. Plots of $Log(I_{emi})$ versus d for different excitation intensities I_{exc} (a) I_o, (b) $0.1 \times I_o$ and (c) $0.01 \times I_o$. The loss factor was found to be 7.3, 5.1 and 8.0 cm^{-1} respectively.

Downloaded From: http://proceedings.spiedigitallibrary.org/ on 05/01/2014 Terms of Use: http://spiedl.org/terms

different from that shown in Fig. 2 because of the difference in the well widths of the MQW samples used, as has been previously observed [10]. The emission peak position of QW transition shows a slight decrease with increase in d. The integrated intensity (I_{emi}) from QW emission decreases with increase in d approximately according to the relationship $I_{emi}(d) = I_o(10^{-\alpha d})$ where α is the loss factor. Fig. 7 Shows plots of $\log(I_{emi})$ versus d for different excitation intensities I_o, 0.1 x I_o and 0.01 x I_o. The loss factor was found to be around 5 - 8 cm^{-1}. The decrease in PL emission intensity with increase in d can be understood in terms of light propagation loss in the waveguides that occurs in many different forms including scattering at the walls of the waveguides and reabsorption. At the spot on the waveguide where initial excitation occurs, carriers and excitons are generated. They recombine and emit light that is laterally confined to propagate along the waveguide. PL emitted at the excitation spot will traverse the distance, d along the waveguide before being detected. The longer the distance the photons have to travel, the more the chance of loss through scattering or reabsorption leading to a decrease in the integrated emission intensity, as seen in Fig. 7. For comparison, we studied waveguides oriented parallel to the collecting slit (not shown) and found that the integrated emission intensity was consistently equal for different laser excitation positions on the waveguide. This is in agreement with the explanation given above.

Fig. 8 shows the temporal response of the PL emission at 3.585 eV, corresponding to the spectral peak position for the waveguide lined perpendicular to the collecting slit. The temporal PL responses were collected under laser excitation from five different positions, d on the same waveguide with fixed excitation conditions. The responses for different d values are similar in slope both in the rise part and the decay part. The decay can be fitted quite well with a single exponential giving a lifetime of 230 ± 2 ps. However, there is a systematic increase in time delay in the initial PL signal buildup as d is increased. This is shown more clearly in the inset of Fig. 8. The arrival times at three different locations labeled A, B, C in Fig. 8 for five laser excitation spot

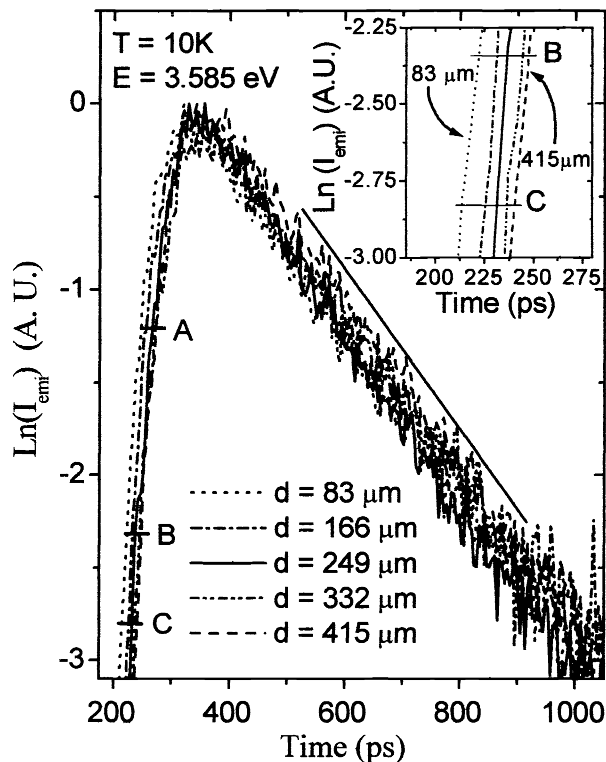

Fig. 8. The temporal responses of the PL emission measured at the spectral peak position (3.585 eV) of a waveguide lined perpendicular to the collecting slit. The responses were collected under laser excitation from five different positions, d of the same waveguide with fixed excitation intensity. The inset shows more clearly the time delay observed in the rise part of the temporal response for the five different values of d, with d = 83 µm on the left and d = 415 µm on the right.

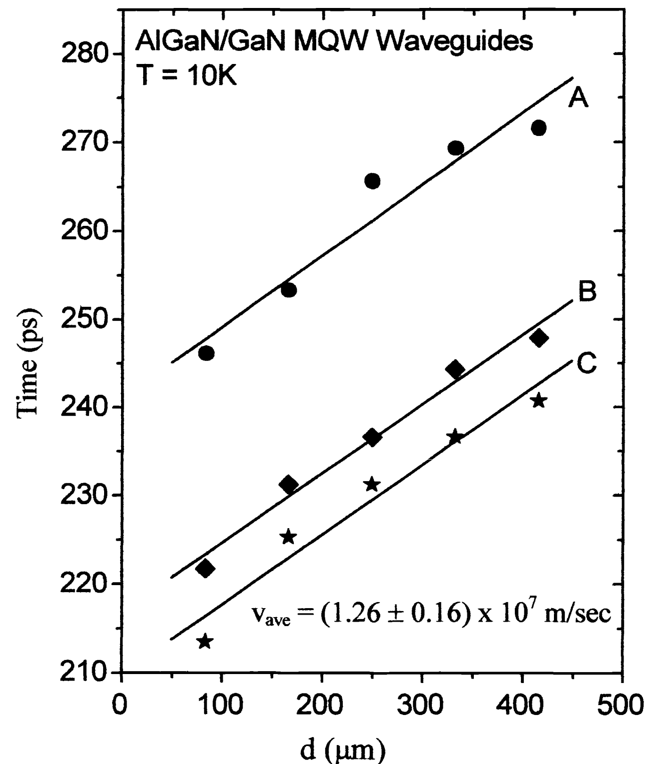

Fig. 9. The variation in time delay with laser excitation spot position d. These delay times were extracted from three locations labeled A, B, C in Fig. 3. Data points are shown in symbols and the lines are the least-square fits of the data points with a linear relation. From these, an average propagation speed of (1.26 ± 0.16) x 10^7 m/sec of light in the waveguide was determined.

Downloaded From: http://proceedings.spiedigitallibrary.org/ on 05/01/2014 Terms of Use: http://spiedl.org/terms

positions d are plotted in Fig. 9. The inverse of the slopes from each of these locations A, B, and C yields an average velocity of $(1.26 \pm 0.16) \times 10^7$ m/sec, which is the propagation speed of generated photons, with energy corresponding to the well transitions in the MQW. Using an approximate value of refractive index n = 2.67 for GaN [13], the speed of light in the waveguide is estimated to be $c/n = 1.12 \times 10^8$ m/sec. This is an order of magnitude greater than the velocity of the generated photons in the waveguides that we have determined.

In direct band gap semiconductors including the group III-nitrides, polaritons, the coupled mode of photons and excitons, is the normal mode of propagation of light in semiconductors in the neighborhood of exciton resonant energy [14]. In a quantum well system, the coupling between excitons and photons to form excitonic polaritons is further enhanced due to the quantum confinement effect [15,16]. A quasi-one dimensional structure such as the waveguide structure we have studied is expected to show even more stable excitonic polaritons because of the increased oscillator strength of excitons [16,17]. We therefore expect that the generated light in the waveguides propagate in excitonic polariton mode. In this mode, the propagation velocity has strong energy dependence particularly in the knee region of the polariton dispersion curve, and is typically much smaller than the speed of light in the semiconductors. The reduced propagation speed of the polaritons in the waveguide is expected since the coupling between the excitons and photons occurs at the energy corresponding to exciton transitions in the MQW. The average speed obtained is a measure of the propagation speed of polaritons inside the waveguide. Polaritons with speeds three or four orders of magnitude slower than the speed of light in different semiconductors in the bottleneck region have been previously observed [14, 18-20].

Our results shed light towards the fundamental physics behind propagation of light in III-nitride semiconductors. This information is important for many device applications. For example, when the ridge-guide laser diode is used as a read/write laser source in digital versatile disks (DVDs), the ridge width has to be reduced to dimensions of micron size in order to obtain fundamental transverse modes necessary to collimate the laser light to a small spot [21]. The knowledge of the speed at which light is propagated along such a device is basic to its design for improved operation.

4. SUMMARY

We have fabricated submicron waveguide structures based on AlGaN/GaN MQWs. The spectral peak and line width of the PL emission line for waveguides fabricated with fixed widths and different orientation was found to have 6-fold symmetry. This variation is most likely due to the anisotropy in carrier or exciton diffusion coefficients. The 60° periodic variation is expected due to the hexagonal crystal structure of the nitride materials. The integrated emission intensity systematically decreases when detected from one end of the waveguide as the laser excitation position on the waveguide is varied. The temporal response also shows a systematic increase in time delay with laser excitation position. These changes in integrated intensity as well as time delay has been explained in terms of propagation of exciton-polaritons in the MQW waveguides of the III-nitride materials. The propagation speed of the polaritons in the knee region of waveguide was determined to be $(1.26 \pm 0.16) \times 10^7$ m/sec.

ACKNOWLEDGEMENTS

The research is supported by DOE (96ER45604/A000), NSF (DMR-9902431 and INT-9729582), ARO, BMDO, and ONR.

REFERENCES

a) E-mail : jiang@phys.ksu.edu

1. H. Morkoc, S. Strite, G. B. Gao, M.E. Lin, B. Sverdlov, and M. Burns, J. Appl. Phys. **76**, 1363 (1994).
2. S. X. Jin, J. Li, J. Z. Li, J. Y. Lin and H. X. Jiang, *Appl. Phys. Lett.* **76**, 631 (2000).
3. K. C. Zeng, L. Dai, J. Y. Lin and H. X. Jiang, *Appl. Phys. Lett.* **75**, 2563 (1999).
4. H. X. Jiang, J. Y. Lin K. C. Zeng and W. Yang, *Appl. Phys. Lett.* **75**, 736 (1999).
5. K. C. Zeng, J. Y. Lin, H. X. Jiang and W. Yang, *Appl. Phys. Lett.* **74**, 1227 (1999).

Downloaded From: http://proceedings.spiedigitallibrary.org/ on 05/01/2014 Terms of Use: http://spiedl.org/terms

6. R. A. Mair, K. C. Zeng, J. Y. Lin, H. X. Jiang, B. Zang, L. Dai, H. Tang, A. Botchkarev, W. Kim, and H. Morkoc, *Appl. Phys. Lett.* **75**, 2563 (2000).
7. http://www.phys.ksu.edu/area/GaNgroup.
8. D. Kapolnek, S. Keller, R. Vetury, R. D. Underwood, P. Kozodoy, S. P. Den Baars and U. K. Mishra, *Appl. Phys. Lett.* **71**, 1204 (1997).
9. H. Asai, *J. Cryst. Growth* **80**, 425 (1987).
10. K. C. Zeng, J. Li, J. Y. Lin and H. X. Jiang, *Appl. Phys. Lett.* **76**, 3040 (2000).
11. K. C. Zeng, M. Smith, J. Y. Lin and H. X. Jiang, *Appl. Phys. Lett.* **73**, 1724 (1998).
12. P. Kung, C. J. Sun, A. Saxler, H. Ohsato and M. Razeghi, *J. Appl. Phys.* **75**, 4515 (1994).
13. U. Tish, B. Meyler, O. Katz, E. Finkman and J. Salzman, *J. Appl. Phys.* **89**, 2676 (2001).
14. Y. Masumoto, Y. Unuma, Y. Tanaka and S. Shionoya, *J. Phys. Soc. Jpn.* **47**, 1884 (1979).
15. T. Katsuyama and K. Ogawa, *J. Appl. Phys.* **75**, 7607 (1994).
16. T. Katsuyama, S. Nishimura, K. Ogawa and T. Sato, *Semicon. Sci. Technol.* **8**, 1226 (1993).
17. M. Matsuura and T. Kamizato, *Surf. Sc.* **174**, 183 (1986).
18. R. G. Ulbrich and G. W. Fehrenbach, *Phys. Rev. Lett.* **43**, 963 (1979).
19. D. E. Cooper and P. R. Newman, *Phys. Rev. B* **39**, 7431 (1989).
20. J. Y. Lin, Q. Zhu, D. Baum and A. Honig, *Phys. Rev. B* **40**, 1385 (1989).
21. S. Nakamura, S. Senoh, S. Nagahama, N. Iwasa, T. Yamada, T. Matsushita, H. Kiyoku, Y. Sugimoto, T. Kozaki, H. Umemoto, M. Sano and K. Chocho, *Appl. Phys. Lett.* **72,** 2014 (1998).

Downloaded From: http://proceedings.spiedigitallibrary.org/ on 05/01/2014 Terms of Use: http://spiedl.org/terms